sustainability

MDPI

Article

Assessment of the Future Changes in the Socio-Economic Vulnerability of China's Coastal Areas

Cuihua Li, Rongshuo Cai * and Xiuhua Yan

Third Institute of Oceanography, Ministry of Natural Resources, Xiamen 361005, China
* Correspondence: cairongshuo@tio.org.cn

Abstract: China's coastal areas are under serious threat of continued sea-level rise, and sustainable coastal development is closely linked to changes in socio-economic vulnerability. To this end, based on the Intergovernmental Panel on Climate Change framework of shared socio-economic pathways (SSPs), this study constructed a system of indicators to assess the socio-economic vulnerability of China's coastal areas in 2030, 2050, and 2100 under low, medium, and high greenhouse gas emission scenarios (SSP1-2.6, SSP2-4.5, and SSP5-8.5, respectively). The results showed the following: (1) the vulnerability of China's coastal provinces, cities, and counties shows an upward trend (ranked SSP5-8.5 > SSP2-4.5 > SSP1-2.6), which is mainly attributed to a continued increase in the exposure of socio-economic systems to sea-level rise and differences in the age structure of the population within the study regions; and (2) areas with higher vulnerability are concentrated in economically developed coastal areas, such as the Bohai Bay Rim and the Yangtze River Delta, Jiangsu, and Pearl River Delta regions, owing to their high proportions of low-lying land, long coastlines, and dense residential areas associated with economic development. Based on these results, climate-resilient solutions are needed to improve socio-economic adaptations for ongoing climate change in China's coastal areas.

Keywords: climate change; coastal vulnerability; socio-economy; sea-level rise; socio-economic pathway scenario

check for updates

Citation: Li, C.; Cai, R.; Yan, X. Assessment of the Future Changes in the Socio-Economic Vulnerability of China's Coastal Areas. *Sustainability* **2023**, *15*, 5794. https://doi.org/10.3390/su15075794

Academic Editors: Pallav Purohit, Xiaodong Yan and Shaohong Wu

Received: 15 March 2023
Accepted: 22 March 2023
Published: 27 March 2023

1. Introduction

The sixth assessment report (AR6) of the Intergovernmental Panel on Climate Change (IPCC) shows that since 1850, the global climate system has been warming continuously, and the last four years have been warmer than any previous year. Compared with the pre-industrialization period (1850–1900), the warming in the first two decades of this century has reached approximately 0.99 °C [1]. Furthermore, in the past hundred years, the global sea level has continued to rise due to the melting of land glaciers caused by climate warming as well as the thermal expansion of the oceans [1,2]. In recent decades, the rise of global and coastal sea levels in China has also accelerated [3,4]. Under the IPCC framework of shared socio-economic pathways (SSPs), by 2100, the global mean sea level is expected to increase by 0.38 and 0.77 m relative to 1995–2014 under low and high greenhouse gas (GHG) emission scenarios (SSP1-2.6 and SSP5-8.5), respectively [1,5]. Over the past 40 years, the sea level around China has shown an accelerated rising trend at an average rate of 3.4 mm/y, which is higher than the global average over the same period [6]. It is estimated that the sea level will continue to rise by 55–170 mm over the next 30 years [7]. This accelerated rise increases the risks posed to low-lying coastal areas and populations, as relatively small increases in sea level will significantly increase the frequency and intensity of floods in these areas [4]. Moreover, sea level rise increases the baseline water level of storm surges, tides, and waves, which further increases the risk of typhoon-driven storm surges and coastal flooding [3,8,9]. Approximately 23% of the world's population lives within 100 km of the coast [10], which is expected to increase to almost 50% by 2030 [11]. In China, more than 70% of the large and medium-sized cities are coastal, accounting for just 13% of the land area but supporting 42% of the country's population and more than 60% of the country's gross domestic product (GDP) [12,13]. China's coastal areas have long been affected by marine disasters including sea-level rise, typhoons, storm surges, seawater intrusion, soil salinization, and saltwater intrusion [7]. Indeed, the high density of socio-economic infrastructure in many of China's coastal areas often generates a series of impacts following marine disasters that seriously threatens human life and production [7]. For example, in the early 1980s, the annual economic loss from marine disasters in China reached more than one billion yuan and increased to approximately 10 billion yuan in every year of the 1990s [7,14]. In the future, China's coastal areas are expected to show continued rapid economic growth, which, when coupled with ongoing global climate change, will lead to an increase in the frequency of natural disasters and associated socio-economic risks [15].

The socio-economic system (here referred to as the "social economy") is a complex mega-system with humans at the core and incorporating social, economic, educational, science and technological, and ecological environmental systems. As a multi-dimensional system, analyzing changes in the social economy can be extremely difficult, and it is usually necessary to adopt dimensional reduction. Here, GDP and population demographics were used to characterize the social economy of China's coastal areas. According to the IPCC [16,17], socio-economic vulnerability can be defined as the tendency or habit of a system to be vulnerable to the adverse impact of climate disaster-causing factors; a state in which a system is vulnerable to damage due to exposure to climate disaster-causing factors and anthropogenic activities, which can also be seen as a result of the joint action of exposure, sensitivity, and adaptability [18,19]. Social vulnerability usually refers to the vulnerable state of social groups and their ability to recover from disasters, which is also reflected by socio-economic conditions and demographic characteristics [20,21]. Social vulnerability assessments are usually based on the establishment of an indicator system, and different mathematical methods can be used to calculate social vulnerability indices. At present, commonly used methods include the comprehensive index [20,22–26] and functional model methods [27–31]. In recent years, geographical information systems have also been widely applied in social vulnerability assessments [32–35].

The comprehensive index method is simple and easy to apply; however, this approach ignores the interactions between the various components of vulnerability. Alternatively, the functional model method better reflects the interactions between the components of vulnerability, which is more conducive to explaining the causes and characteristics of vulnerability [36]. However, owing to differences in the understanding of the components of social vulnerability, the application of these models varies greatly.

Previous research shows that with ongoing sea-level rise, the overall vulnerability of China's coastal areas increased between 2006 and 2016 but remained stable in some areas. For example, the vulnerability of coastal areas in East and South China is higher than that of coastal areas in North and Northeast China [30,37]. There is also evidence that the highest levels of social vulnerability are concentrated in Hainan Province and the coastal areas of the Beibu Gulf, with the north coast of Jiangsu Province and Liaoning Province also showing high vulnerability [25]. Most studies on social vulnerability in coastal areas use provincial and municipal administrative regions as assessment units [29,35], and studies on county-level administrative regions have tended to focus on specific regions, such as the Yangtze River Delta [38,39] and the Yellow River Basin [26]. Furthermore, while previous studies have mainly focused on historical changes in social and economic vulnerability, the potential response of China's social economy under future climate scenarios remains understudied.

Crucially, future socio-economic risk depends on the interaction between the hazard posed by climate disaster-causing factors and the exposure, sensitivity, and adaptability of the system. Therefore, research on future socio-economic vulnerability has become critical for risk assessment. In this study, the social economy of China's coastal provinces, cities, and counties was examined using a social economic vulnerability assessment index based on exposure, sensitivity, and adaptability under three IPCC SSP scenarios, namely SSP1-2.6, SSP2-4.5, and SSP5-8.5 (collectively referred to as SSPx-y) [1,17]. These scenarios consider three representative concentration pathways (RCP2.6, 4.5, and 8.5; collectively referred to as RCPs) corresponding to low, medium, and very high GHG emissions, and three corresponding SSPs, namely a sustainable path, intermediate path, and fossil fuel-based development path (SSP1, 2, and 5, respectively). Adopting such a scenario-based approach enables the assessment of future socio-economic vulnerability, which provides valuable evidence to support the development of climate change adaptation strategies.

2. Data and Methods

2.1. Study Area

China's coastal areas include areas with mainland and island coastlines, which are divided into coastal provinces, autonomous regions, and municipalities under the Central Government according to administrative regions. China has nine coastal provinces, one autonomous region, two municipalities directly under the Central Government, 53 coastal cities, and 242 coastal counties. Considering the availability of data, the coastal areas referred to in this paper include 11 provincial administrative regions, including Tianjin, Shanghai, Jiangsu, Guangdong, and other coastal provinces; municipalities directly under the Central Government; autonomous regions (excluding Hong Kong, Macao, and Taiwan); 62 municipal administrative regions; and 212 county-level administrative regions (Figure 1). In addition, as Hainan Island is surrounded by sea, only Haikou and Sanya are municipal administrative regions. Thus, county-level administrative regions along the coast of Hainan Province were included in the evaluation scope of the municipal administrative regions.

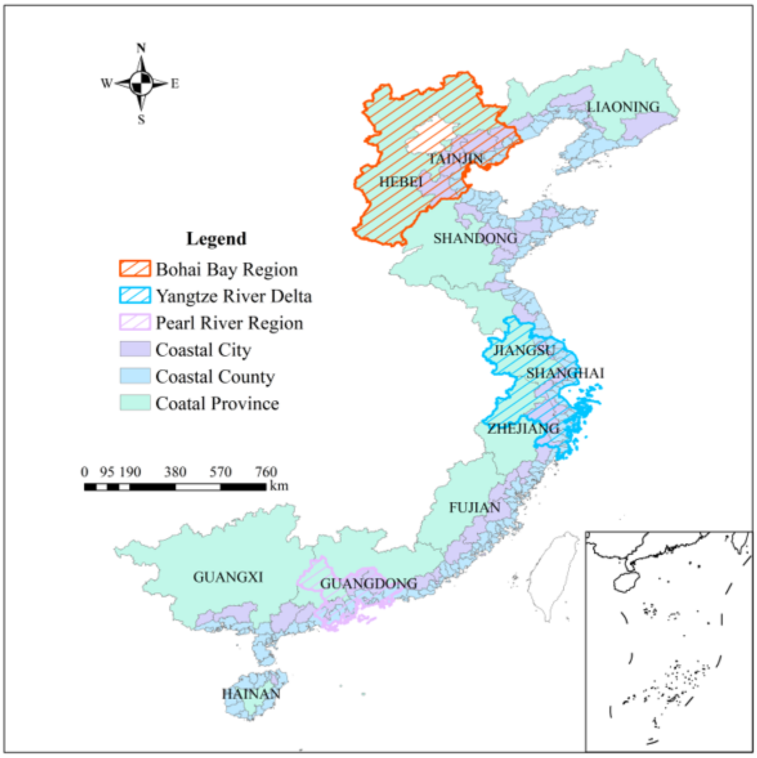

Figure 1. Map of China's coastal areas.

2.2. Data Sources

2.2.1. Environmental Data

(1) Digital elevation model data were derived from the Shuttle Radar Topography Mission digital elevation dataset, jointly completed by the National Aeronautics and Space Administration and the National Imagery and Mapping Agency, covering the land area

60° N–60° S and with a resolution of 90 m (https://srtm.csi.cgiar.org/ (accessed on 1 September 2020).

(2) The coastline and area data of the coastal administrative regions were obtained from the 2010 China Statistical Yearbook and statistical yearbooks of 11 coastal provinces, municipalities, and autonomous regions (http://www.stats.gov.cn/tjsj/ndsj/ (accessed on 21 October 2020) [40].

(3) The model results of the Fifth International Coupled Model Comparison Plan (CMIP5), including 29 models such as CMCC-CM, CNRM-CM5, and MIROC-ESM, were selected for the sea-level rise prediction data. These data consisted of sea-level height simulations for coastal areas from 2030 to 2100 under the different RCP scenarios, for which estimated future sea-level rise was obtained as multi-year weighted averages [41].

2.2.2. Socio-Economic Data

(1) Historical population data were derived from the sixth national population census released by the National Bureau of Statistics in 2011, incorporating detailed data on population size, age structure, and other classifications for each sub-county in the target coastal areas (http://www.stats.gov.cn/ztjc/zdtjgz/zgrkpc/dlcrkpc/ (accessed on 13 January 2021).

(2) Historical socio-economic assessment was based on the GDP of all cities in China in 2010, as released by the National Bureau of Statistics (https://data.stats.gov.cn/easyquery.htm?cn=C01 (accessed on 13 January 2021).

(3) Population and GDP data for the coastal areas of China between 2010 and 2100 were simulated under three SSPs. The time-step of the data outputs was 10 years, and the spatial resolution was 0.5 km × 0.5 km (https://nsem.bnu.edu.cn/gjgcs/120719.htm (accessed on 23 July 2021) [42,43].

2.3. Research Methods

2.3.1. Socio-Economic Vulnerability Index

The socio-economic vulnerability index adopted in this study was used to measure the degree of socio-economic loss under the impact of climate change disaster-causing factors (i.e., sea-level rise). For this, vulnerability (V) is composed of system exposure (E), sensitivity (S), and adaptability (A) [19,44,45]; E refers to the intersection of adverse impact scope and system distribution in space when climate disaster-causing factors occur; S refers to the inherent attribute (nature) that the system experiences when facing climate change disaster-causing factors and anthropogenic disturbance, which reflects the degree to which the system can withstand disturbance; and A refers to the ability of a system to cope with climate change and anthropogenic disturbance as well as the ability to recover from damage. Based on the IPCC comprehensive risk theory of climate change, following the principles of selecting indicators based on representativeness, operability, and accessibility, and referring to previous research [20,25,26,46], a socio-economic vulnerability assessment index was constructed using E, S, and A as three first-level assessment indicators, with secondary evaluation indicators determined as shown in Table 1.

Table 1. Components of a socio-economic vulnerability index for China's coastal areas [20,25,26,46].

Level I Indicators	Secondary Indicators	Index Meaning	Description and Calculation
Exposure (E)	Proportion of low-lying land area ($E1$)	Area of low-lying land/administrative area with elevation < 10 m	$E_{1i} = \frac{D_i}{M_i}$, (1) where i is the ith evaluation unit; D is the area of the assessment unit with an elevation < 10 m, and M is the area of the assessment unit.
	Coastline length/assessment unit ($E2$)	Ratio of coastline length to assessed area	$E_{2i} = \frac{L_i}{M_i}$, (2) where i is the ith evaluation unit; L is the coastline length of the assessment unit, and M is the area of the assessment unit.

Table 1. *Cont.*

Level I Indicators	Secondary Indicators	Index Meaning	Description and Calculation
	Relative sea level height (*E*3)	Relative sea level height along the coast of the assessment unit	Statistical analysis using spatial analysis tools in ArcGIS.
	Total population (*E*4)	Total population in the assessment unit	Statistical analysis using spatial analysis tools in ArcGIS.
	Total GDP (*E*5)	Total GDP in the assessment unit	Statistical analysis using spatial analysis tools in ArcGIS.
Sensibility (*S*)	Proportion of elderly population (*S*1)	Proportion of the elderly aged over 60	$S_{1ij} = \frac{C_{ij}}{P_{ij}}$, (3) where i is the ith evaluation unit, and j represents the year; C refers to the elderly population over 60 years old in the assessment unit, and P refers to the total population in the assessment unit.
	Proportion of adolescent population (*S*2)	Proportion of young people under 14 years old	$S_{2ij} = \frac{Q_{ij}}{P_{ij}}$, (4) where i is the ith evaluation unit, and j represents the year; Q is the population of adolescents under 14 years old in the assessment unit, and P is the total population in the assessment unit.
	Population density (*S*3)	Population per unit area	Statistical analysis using spatial analysis tools in ArcGIS.
Adaptability (*A*)	Proportion of labor force population (*A*1)	Proportion of labor force aged 15–59	$A_{2ij} = \frac{N_{ij}}{P_{ij}}$, (5) where i is the ith evaluation unit, and j represents the year; N is the labor force population aged 15–59 in the assessment unit, and P is the total population in the assessment unit.
	Economic density (*A*2)	Unit area GDP	Statistical analysis using spatial analysis tools in ArcGIS.

Exposure reflects socio-economic exposure to disasters including sea-level rise and typhoon-driven storm surges; the higher the exposure of an area, the higher is its vulnerability. Notably, levels of exposure have increased with sea-level rise and the ongoing socio-economic development in coastal areas. Specifically, the exposure of coastal areas is closely related to changes in the relative sea level, the proportion of low-lying land, and the length of the coastline/administrative area as well as other factors [47–49]. Sensitivity is closely linked to population density and structure. Here, population density and the proportions of younger and elderly people were used to represent *S*, as these metrics are associated with greater social impact during disasters [25,47]. Adaptability reflects resilience in the face of climate disaster-causing factors; the higher the adaptability of the population, economy, education, and infrastructure, the lower is the social vulnerability. Thus, *S* is positively correlated with socio-economic vulnerability while *A* is negatively correlated. Owing to a lack of data for future levels of education, urbanization, medical security, and other factors, GDP per unit area and the labor population ratio were used to represent socio-economic adaptability. In addition, because economic density is an indicator of both social and economic adaptability, higher and lower economic density represents higher and lower degrees of vulnerability to disasters, respectively. Therefore, economic density was applied as one of the components of *A*, with a weighting of 0.51 based on the entropy method (Table 1).

2.3.2. Computing Methods

According to the relationships between vulnerability and the relevant constituent factors, and referring to the expression mode of the vulnerability function proposed by Luna et al. [50], a series of social and economic vulnerability assessment models for China's coastal areas was constructed, as follows:

$$\text{Exposure indexcalculation model}: \ E = \sum_{i=1}^{n} E_i b_i, \tag{6}$$

where E is the exposure index, E_i is the ith index of exposure, b_i is the weight coefficient of the ith exposure index, and n is the number of exposure indices.

$$\text{Sensitivity index calculation model}: \ S = \sum_{i=1}^{n} S_i c_i, \tag{7}$$

where S is the sensitivity index, S_i is the ith sensitivity index, c_i is the weight coefficient of the ith sensitivity index, and n is the number of sensitivity indices.

$$\text{Adaptability index calculation model}: \ A = \sum_{i=1}^{n} A_i d_i, \tag{8}$$

where A is the adaptability index, A_i is the ith index of adaptability, d_i is the weight coefficient of the ith adaptability index, and n is the number of adaptability indices.

$$\text{Vulnerability index: } V = E + S - A, \tag{9}$$

where V is the vulnerability index, E is the exposure index, S is the sensitivity index, and A is the adaptability index.

Existing research shows that the two calculation approaches $V = E + S - A$ and $V = E \cdot S/A$ do not generate significant differences in the vulnerability equivalent sequence [44,51], while the numerical range of the calculation results based on the former approach is smaller, more intuitive, and conducive to comparison. Therefore, the more commonly applied addition and subtraction expression was adopted here.

Because there are differences in magnitude, dimension, and index properties between different evaluation indicators, a standardization procedure was applied to divide the original data of the selected evaluation indicators by the maximum value. Based on this, the objective entropy method was used to determine the weights of each indicator [44].

The secondary indicators of exposure, sensitivity and adaptability are 5, 3, and 2 respectively, thus the vulnerability index is not balanced, because exposure is more important than sensitivity and adaptability to determine vulnerability. To solve this problem, the weight of exposure, sensitivity, and adaptability is determined as 1, and then the weight of secondary evaluation indicators is determined according to the entropy method. In order to judge the stability of the socio-economic vulnerability assessment model, it is necessary to conduct a sensitivity analysis on the indicator weight and study the impact of the change of weight on the assessment results. Using the index weight sensitivity analysis method in the literature [52,53], the weight sensitivity analysis results are obtained. See Table 2. If we want to maintain the stability of socio-economic vulnerability, that is, the order of vulnerability ranking remains unchanged and the change interval of the weight are as follows: $c_1 < b_1 < c_2 < b_2 < b_4 < d_1 < b_3 < d_2 < b_5 < c_3$. The weight change interval of proportion of adolescent population is the smallest and the sensitivity is the largest, while population density, total GDP, economic density, and relative sea level height have a relatively large weight change range and a relatively small sensitivity. The weight sensitivity is generally low, so the socio-economic vulnerability evaluation method selected in this paper is stable and the evaluation results are reliable.

Table 2. Components of a socio-economic vulnerability index for China's coastal areas.

Evaluation Indicators		Weight	Weight Change Threshold		Range
Proportion of low-lying land area	b_1	0.37	0.241	0.463	0.222
Coastline length/assessment unit	b_2	0.16	0.088	0.336	0.248
Relative sea level height	b_3	0.14	0.063	0371	0.308
Total population	b_4	0.18	0	0252	0.252
Total GDP	b_5	0.15	0	0.345	0.345
Proportion of elderly population	c_1	0.15	0.113	0.225	0.112
Proportion of adolescent population	c_2	0.2	0.190	0.430	0.240
Population density	c_3	0.65	0.520	0.943	0.423
Proportion of labor force population	d_1	0.21	0	0.294	0.294
Economic density	d_2	0.79	0.672	0.988	0.316

2.3.3. Evaluation Indicator Grading

As there is no consistent standard for the classification of social vulnerability, the quantile grading method was applied in ArcGIS to divide the socio-economic vulnerability scores into five levels—very high, high, medium, low, and very low (Table 3).

Table 3. Classification of socio-economic vulnerability (V) in China's coastal areas.

Evaluation Unit	Very High	High	Medium	Low	Very Low
Province	>0.61	0.43–0.61	0.30–0.43	0.21–0.30	≤0.21
City	>0.52	0.29–0.52	0.19–0.29	0.07–0.16	≤0.07
County	>0.55	0.33–0.55	0.18–0.33	0.09–0.18	≤0.09

3. Results and Discussion

3.1. Socio-Economic Vulnerability

3.1.1. Coastal Provinces

The results of the socio-economic vulnerability assessment for China's coastal provincial administrative areas under the different climate change scenarios are summarized in Figure 2 and Table 4. Given that areas with a comparable intensity of disaster-causing factors and higher vulnerability are more likely to suffer social and economic losses, regions with a medium or higher level of vulnerability level were of greatest interest. In 2010, vulnerability was low overall, although there were notable regional differences. Shanghai was the only very highly vulnerable area. Jiangsu has a medium level of vulnerability; Tianjin, Shandong, and Guangdong had low vulnerability; Liaoning, Hebei, Zhejiang, Fujian, Guangxi, and Hainan had very low vulnerability, accounting for more than half of all the coastal provincial-level administrative regions.

Under the different SSPx-y scenarios, socio-economic vulnerability showed a general upward trend between values for 2030, 2050, and 2100. Under SSP1-2.6, Shanghai is expected to remain highly vulnerable by 2030, while Tianjin and Jiangsu will increase from low- and medium-vulnerability areas, respectively, to highly vulnerable areas. Shandong, Zhejiang, and Guangdong increase to medium vulnerability areas over the same timeframe, while Hebei and Hainan become low-vulnerability areas, and Liaoning, Fujian, and Guangxi show very low vulnerability. By 2050, Shanghai will maintain a high level of vulnerability, whereas the vulnerability category will increase for other regions, from medium to high for Guangdong, from low to medium for Hainan, and from very low to low for Liaoning and Fujian. By 2100, the vulnerability of Guangxi is also expected to increase from very low to low.

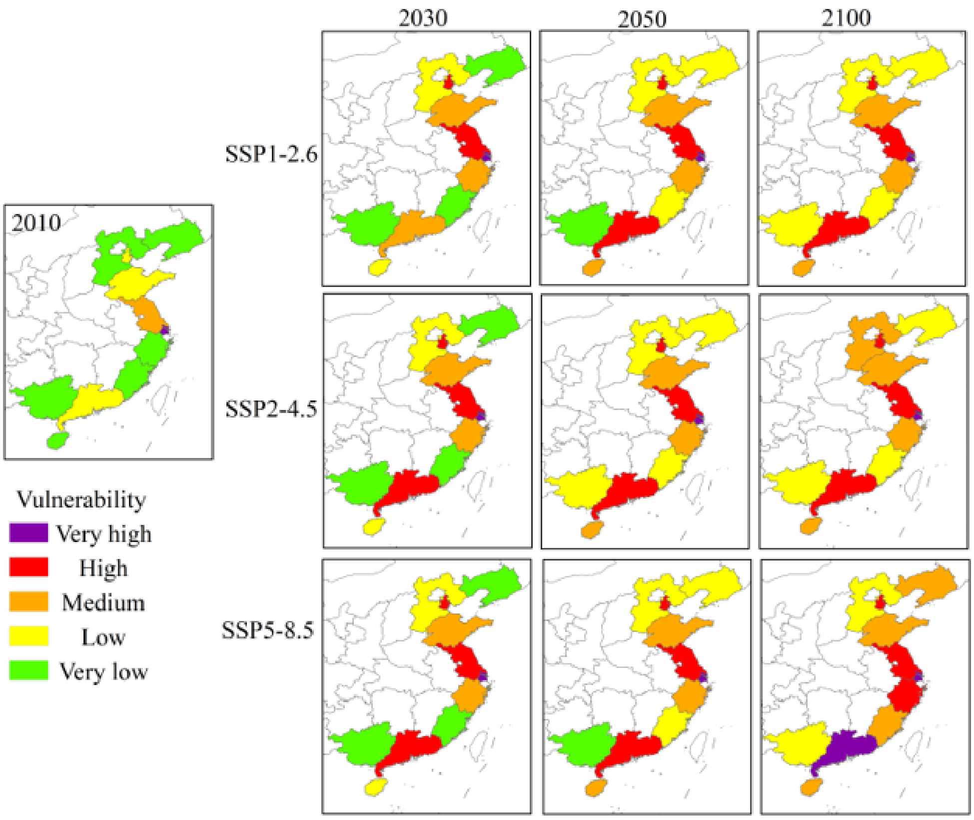

Figure 2. Distribution and evolution of the socio-economic vulnerability of China's coastal provincial administrative regions under different climate scenarios.

Table 4. Changes in the socio-economic vulnerability of China's coastal provincial administrative regions under different climate scenarios.

Vulnerability		**SSP1-2.6**			**SSP2-4.5**			**SSP5-8.5**		
	2010	**2030**	**2050**	**2100**	**2030**	**2050**	**2100**	**2030**	**2050**	**2100**
Very High	1	1	1	1	1	1	1	1	1	2
High	0	2	3	3	3	3	3	3	3	3
Medium	1	3	3	3	2	3	4	2	3	4
Low	3	2	3	4	2	4	3	2	3	2
Very low	6	3	1	0	3	0	0	3	1	0

Under SSP2-4.5, Shanghai is expected to be very highly vulnerable by 2030; Tianjin, Jiangsu, and Guangdong will become highly vulnerable areas; Shandong and Zhejiang will become medium-vulnerability areas; Hebei and Hainan will become low-vulnerability regions; Liaoning, Fujian, and Guangxi will show very low vulnerability. By 2050, there will be no areas with very low vulnerability along the entire coast of China; Hainan will increase to a medium-vulnerability area, while Liaoning, Fujian, and Guangxi will become low-vulnerability areas. By 2100, Hebei will also become a medium-vulnerability area.

The vulnerability results under SSP5-8.5 are similar to those under SSP2-4.5. For example, by 2050, Hainan will become a medium-vulnerability area, and Liaoning and Fujian will show low vulnerability. By 2100, in addition to Shanghai, the vulnerability of Guangdong will increase from high to very high; that of Zhejiang will increase from medium to high; that of Liaoning and Fujian will increase from low to medium; that of Guangxi will increase from very low to low. Notably, there are no areas with very low vulnerability by 2100 under this scenario (Table 4).

3.1.2. Coastal Municipalities

The distribution and evolution of the socio-economic vulnerability of China's coastal municipal administrative regions in 2030, 2050, and 2100 under the different scenarios are shown in Figure 3 and Table 5. In 2010, vulnerability was low overall, although as with the provincial-level results, there were notable regional differences. For example, Shanghai was very highly vulnerable, and highly vulnerable areas were concentrated in Tianjin and Cangzhou around Bohai Bay, Jiaxing, Nantong, and Yancheng in the Yangtze River Delta region, and Shenzhen and Shantou in the Pearl River Delta region. Medium vulnerability areas were concentrated in the coastal cities around Bohai Bay, Jiangsu, and Guangdong; low vulnerability areas were concentrated in the coastal cities of the Shandong Peninsula, Zhejiang, Guangdong, and Guangxi; and very low vulnerability areas were concentrated in Liaoning. The coastal cities in Fujian and Hainan, and almost half of the coastal cities in the whole of China, showed a low level of socio-economic vulnerability.

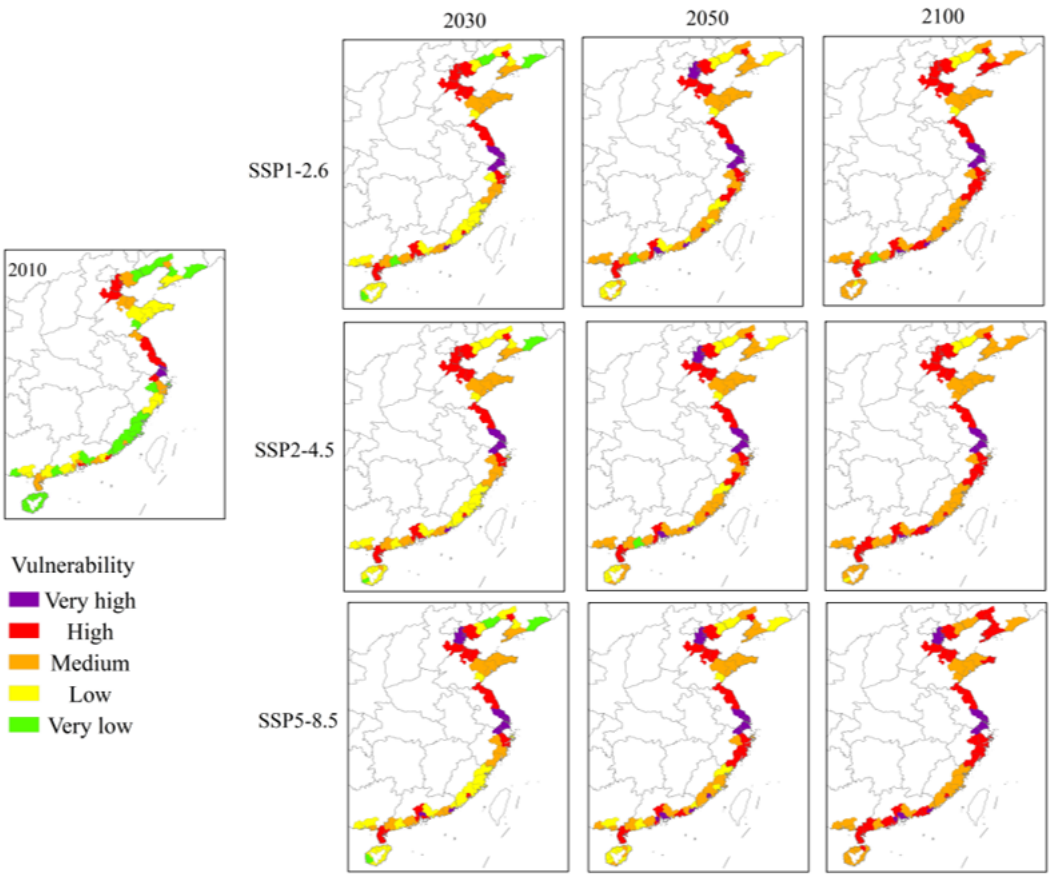

Figure 3. Distribution and evolution of the socio-economic vulnerability of China's coastal municipalities under different climate scenarios.

Table 5. Changes in the socio-economic vulnerability of China's coastal municipalities under different climate scenarios.

Vulnerability	2010	SSP1-2.6			SSP2-4.5			SSP5-8.5		
		2030	2050	2100	2030	2050	2100	2030	2050	2100
Very High	1	4	7	5	4	7	5	6	9	8
High	7	15	14	20	15	14	20	13	14	25
Medium	11	13	23	32	15	27	34	14	21	29
Low	14	25	17	5	26	13	3	25	18	0
Very low	29	5	1	0	2	1	0	4	0	0

Under the different SSPx-y scenarios, the vulnerability of coastal municipal administrative regions showed a general upward trend up to 2100. Under SSP1-2.6, the Bohai Bay Rim, the Yangtze River Delta and Jiangsu coastal areas, the Pearl River Delta, and the Leizhou Peninsula in Guangdong showed significant increases in vulnerability by 2030. For example, Nantong, Jiaxing, and Shantou will be highly vulnerable areas. The number of highly vulnerable areas will increase from 7 to 15, concentrated in Bohai Bay, the Pearl River Delta region, and the Leizhou Peninsula in Guangdong, including Tianjin and sub-provincial cities such as Ningbo, Xiamen, Shenzhen, and Guangzhou. Over the same timeframe, 13 medium-vulnerability areas will be classified in the Shandong Peninsula area, Zhejiang, and some coastal cities in Guangdong; 25 areas show low vulnerability and five show very low vulnerability, particularly in Liaoning, Fujian, Guangxi, and some coastal cities in Hainan. By 2050, vulnerability is expected to increase further, with Tianjin, Shenzhen, and Dongguan classified as having very high vulnerability, and 14 areas classified as having high vulnerability including Wenzhou and Zhuhai. The number of medium-vulnerability areas will also increase to 23, with these areas concentrated in the Liaoning Peninsula region, the Shandong Peninsula region, and mainland coastal cities south of the Yangtze River Delta. Seventeen areas will have low vulnerability, and just one area will have very low vulnerability by 2050. By 2100, Tianjin and Dongguan will show a reduction in vulnerability from very high to high, but the number of highly vulnerable and moderately vulnerable areas will increase significantly, by six and nine, respectively, and there will be no very low-vulnerability areas.

The trends in the socio-economic vulnerability of the coastal municipalities under SSP2-4.5 were consistent with those under the SSP1-2.6 scenario. For example, the number and spatial distribution of areas classified as having very high and high vulnerability were the same between these two scenarios (Table 5), although more medium-vulnerability areas are predicted under SSP2-4.5. Under the SSP5-8.5 scenario, with the exception of some very high-vulnerability areas around Bohai Bay, the vulnerability results are generally consistent with those of SSP1-2.6 and SSP2-4.5.

3.1.3. Coastal Counties

The socio-economic vulnerability of China's coastal county-level administrative regions under the different SSPx-y scenarios is summarized in Figure 4 and Table 5. In 2010, 64.2% of the 212 coastal counties had a low or very low level of vulnerability, 27.3% were medium-vulnerability areas, and only 8.5% were high- and very high-vulnerability areas. The area with the highest vulnerability was Pudong New Area in Shanghai, and other highly vulnerable areas were concentrated in the coastal counties around Bohai Bay, the Yangtze River Delta region, and the Pearl River Delta region, while the moderately vulnerable areas were concentrated in coastal areas around Bohai Bay and Jiangsu.

Under the three SSPx-y scenarios, the socio-economic vulnerability of China's coastal counties is expected to increase, with no very low-vulnerability areas by 2100. Under SSP1-2.6, very highly vulnerable areas will be concentrated along the Yangtze River Delta and the Pearl River Delta regions in 2030 and 2050, and highly vulnerable areas will be concentrated along the Bohai Bay Rim and Yangtze River Delta and Pearl River Delta regions. By 2100, the socio-economic vulnerability of northern Jiangsu is expected to increase significantly, becoming a highly vulnerable area, and the number of very high-vulnerability classifications increases to 73 (Table 6).

Under the SSP2-4.5 scenario, some coastal counties in the Yangtze River Delta and Pearl River Delta regions are expected to be very highly vulnerable by 2030, with highly vulnerable areas concentrated around Bohai Bay and the Yangtze and the Pearl River Deltas. By 2050, there will also be areas with very high vulnerability around Bohai Bay, and by 2100, the number of highly vulnerable areas around Bohai Bay and the Pearl River Delta will decrease, the highly vulnerable areas in the Yangtze River Delta will increase, and Jiangsu will be classified as a highly vulnerable area (Figure 4). Finally, under SSP5-8.5, similar vulnerability classifications are obtained to those under SSP2-4.5. For example, by 2030, 2050, and 2100, 7, 19, and 33 counties will be classified as having very high vulnerability, and 56, 55, and 74 will be classified as highly vulnerable, respectively (Table 6).

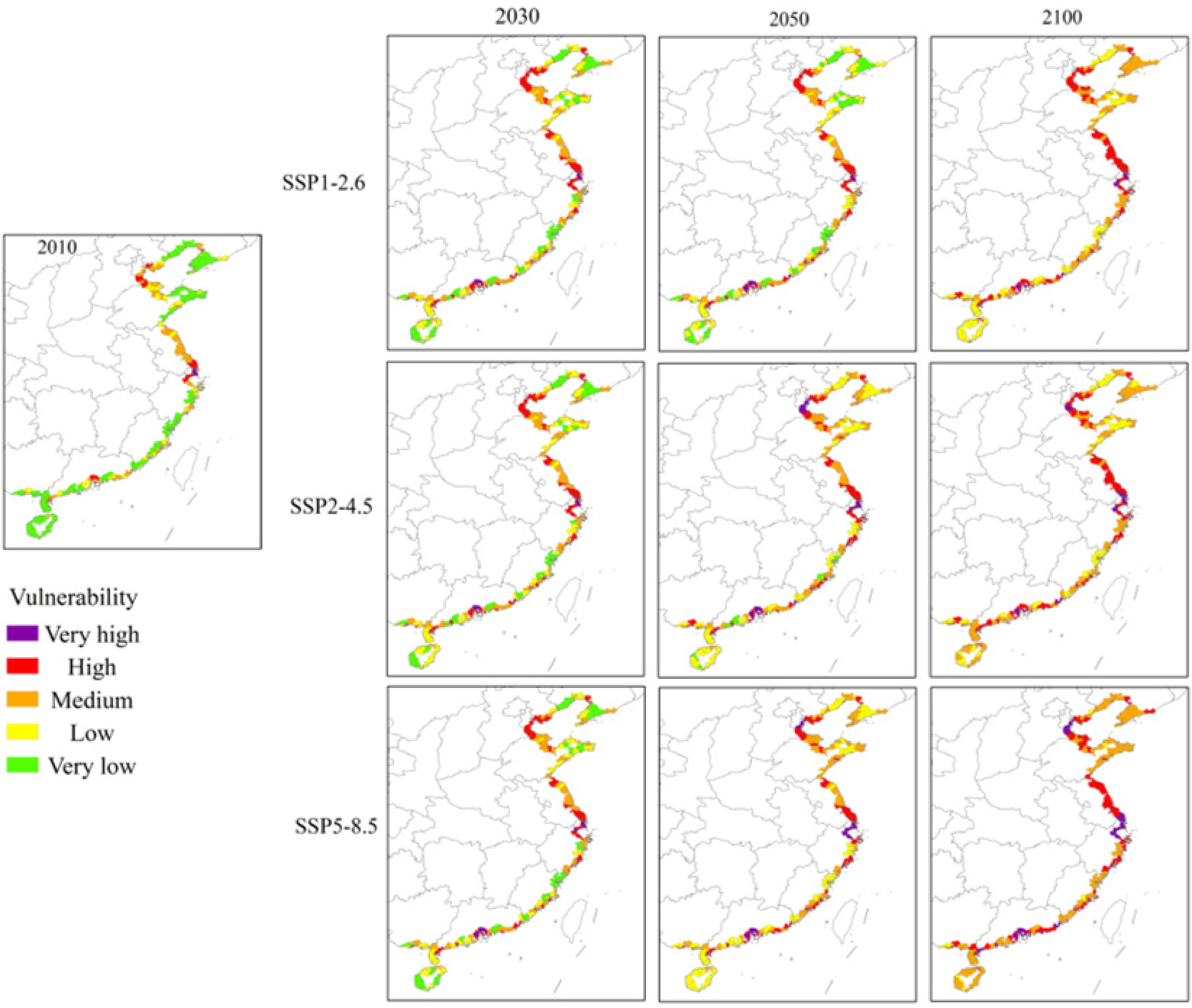

Figure 4. Distribution and evolution of the socio-economic vulnerability of China's coastal county administrative areas under different climate scenarios.

Table 6. Changes in the socio-economic vulnerability of China's coastal county administrative areas under different climate scenarios.

Vulnerability		**SSP1-2.6**			**SSP2-4.5**			**SSP5-8.5**		
	2010	**2030**	**2050**	**2100**	**2030**	**2050**	**2100**	**2030**	**2050**	**2100**
Very High	1	3	9	12	4	17	18	7	19	33
High	17	55	53	73	57	67	70	56	55	74
Medium	58	70	63	80	70	67	85	66	69	99
Low	49	47	51	47	49	53	39	48	48	6
Very low	87	37	36	0	32	8	0	35	10	0

3.2. Socio-Economic Adaptation

The natural environment, population, and social economy are the main factors affecting patterns of socio-economic vulnerability and risk [54]. By identifying China's coastal areas that are highly vulnerable to climate change, suitable adaptive countermeasures can be developed. Based on the results outlined in Section 3.1, the overall socio-economic vulnerability of China's coastal provinces, cities, and counties will increase over the rest of this century, with the areas of highest vulnerability concentrated in Bohai Bay, the Yangtze River Delta region, the coastal areas in northern Jiangsu to the north of the Yangtze River, and the Pearl River Delta region. To better understand vulnerability in these high-risk areas, the key drivers and potential adaptation strategies are further considered in the following sections.

3.2.1. Vulnerability Attribution

Under the three SSPx-y scenarios, the sea level around China's coastal areas will rise significantly by 2030, 2050, and 2100 (Figure 5). This will exacerbate the effects of typhoons, storm surges, coastal floods, and other disaster-causing events, especially in low-lying areas [3,4,55]. Coastal urbanization will further accelerate in the future, increasing the exposure of China's coastal social economy to risk. Furthermore, China's aging population will lead to a shortage of labor in coastal areas and a weakening of socio-economic adaptability [56]. In the vulnerability models, with the continuous emission of GHGs and the intensification of climate warming, increases in relative sea level are associated with increased socio-economic exposure. For example, Figure 5 shows that under the RCP2.6, 4.5, and 8.5 scenarios, sea-level rise remains relatively limited up to 2030, while increases become more pronounced after 2030. The Yangtze River Delta region, Leizhou Peninsula, and Hainan are projected to experience the largest rise in sea level, with likely increases in associated exposure to socio-economic risks. Notably, low-lying coastal areas (<10 m above sea level), population, and economic activity are all concentrated in the coastal areas of the Bohai Bay Rim and the Yangtze River Delta and Pearl River Delta regions (Figure 6). The aging population in these and other coastal areas also increases the sensitivity of the social economy to sea-level-driven risks under SSP1-2.6, 2-4.5, and SSP5-8.5. Thus, the modeled increases in the vulnerability of China's coastal areas over the rest of the century are associated with continuous sea-level rise and changes in the population structure that will increase the exposure and sensitivity and decrease the adaptability of the social economy.

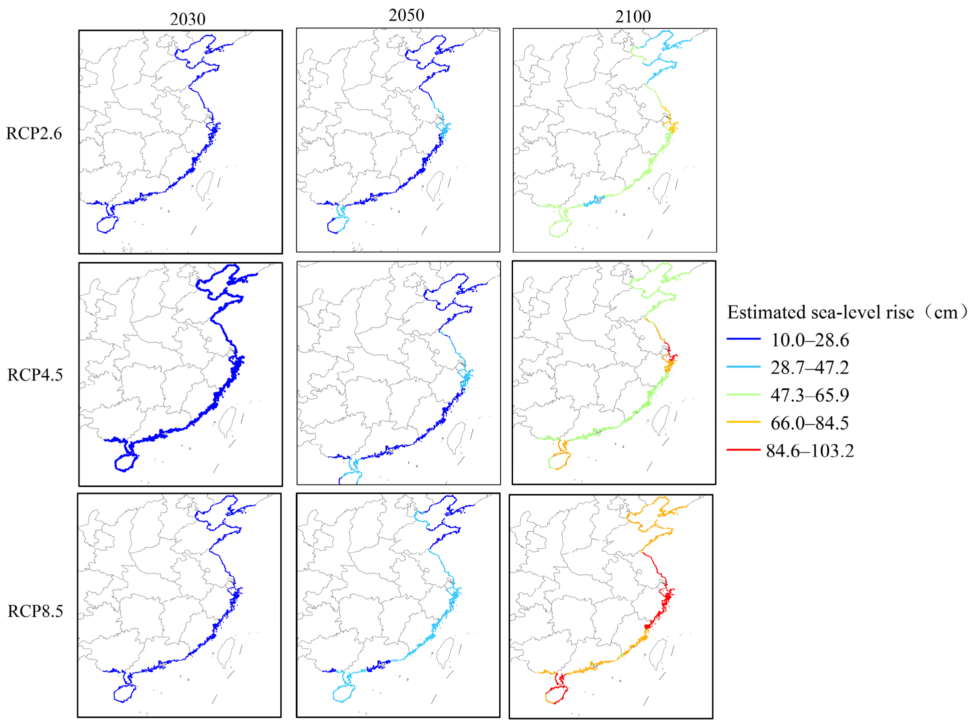

Figure 5. Estimated sea-level rise in China compared with 2000 under different RCP scenarios (Unit: cm).

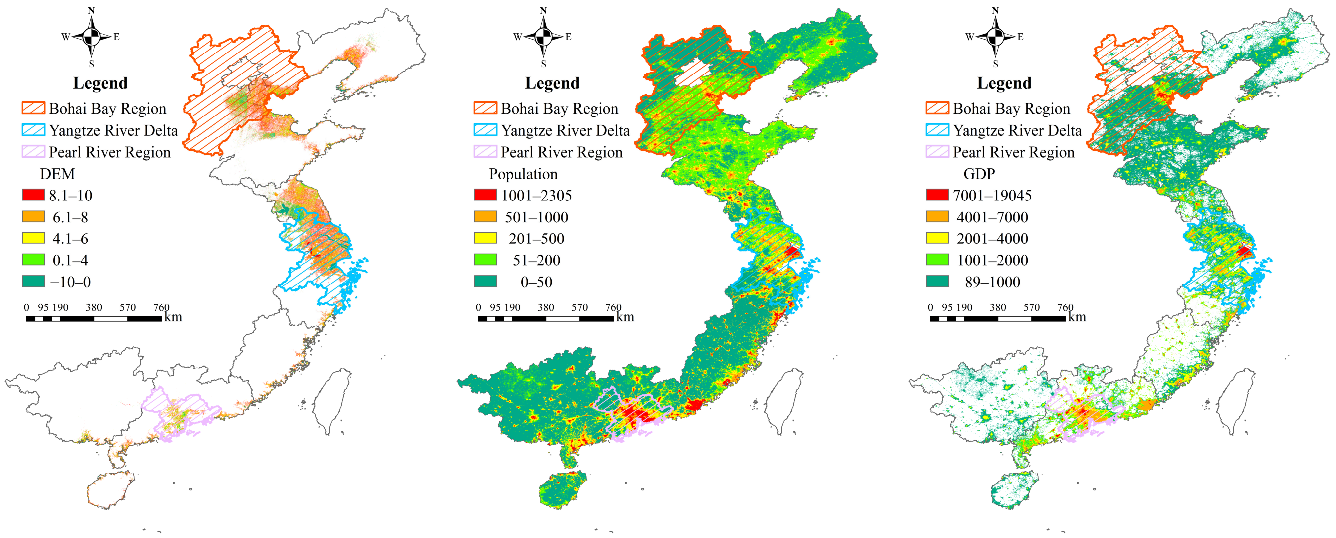

Figure 6. Distribution of low-lying land, population, and gross domestic product (2050 under SSP2-4.5 scenario) in China's coastal areas.

3.2.2. Potential Adaptation Strategies

(1) Improve damp-proofing, flood control, and drainage practices to reduce the exposure risk in coastal areas

Ongoing sea-level rise will increase the exposure of low-lying coastal areas to risk by raising the baseline water level and making what is currently the 100-year extreme coastal water level a multi-year return period in many regions by 2050 and 2100 [4,55]. This poses significant socio-economic risks, especially in large coastal cities [55]. This also implies that coastal protection projects with 50-year and 100-year design lives will not meet the future requirements for flood control and waterlogged land drainage in some coastal areas. Therefore, it is necessary to adjust coastal engineering design standards for flood control and storm surge prevention based on relative sea-level change and improve coastal engineering defense capabilities via reinforcement and upgrading measures to reduce exposure to socio-economic hazards.

Under the SSP5-8.5 scenario, by 2100, the projected sea-level increase affecting China's coastline is an average of at least 66 cm, with greatest increases along the coast from Jiangsu to Zhejiang, near the Leizhou Peninsula in Guangdong, and in northern and eastern coastal areas of Hainan; here, sea level is expected to rise by 84.6–103.2 cm (Figure 5). For these areas, the heights of coastal flood control infrastructure will need to be increased to reflect the projected increase in the base sea level. In addition, to adapt to the changes caused by sea-level rise, river regulation must be strengthened in highly and very highly vulnerable areas to improve the drainage capacity of river courses and improve the foundation design and elevation of protective dikes, sewer pipes, roads, and other critical infrastructure.

(2) Strengthen industrial structures and the layout of low-lying areas to reduce the vulnerability of coastal areas

The coastal areas of China are low and flat, especially in the Bohai Bay Rim, Yangtze River Delta, Jiangsu, and Pearl River Delta areas (Figure 6). These areas are also highly urbanized, densely populated, and economically developed, making them highly vulnerable. In the context of climate change, even if effective measures are taken to mitigate sea-level rise by 2100, there will still be many coastal areas below the average sea level. Therefore, urban planning in coastal areas must adhere to the principle of land and sea integration, fully consider sea-level rise projections, avoid the concentration of residential and high-GDP industries in low-lying coastal areas wherever possible, promote the transfer of important industries inland, and further the urbanization of inland areas. Such measures will help reduce the socio-economic sensitivity of China's coastal areas.

(3) Control GHG emissions to limit climate disaster-causing factors

Under the low (SSP1-2.6), medium (SSP2-4.5), and high (SSP5-8.5) scenarios, the socio-economic vulnerability of China's coastal areas increases proportionally. However, the rate of climate warming and sea-level rise can be slowed by reducing the emission of GHGs. Strengthening the restoration of coastal mangroves, seaweed beds, saltmarshes, and other blue carbon ecosystems alongside the construction of coastal carbon sinks can also play an important role in mitigating climate change.

(4) Improve observation, prediction, and early warning systems for sea-level rise to improve the adaptability of coastal areas

Strengthening and improving the observation, prediction, and early warning systems for sea-level rise hazards, including extreme water levels, and establishing an evaluation system for critical resources, environmental and socio-economic impacts, and countermeasures will increase the adaptability of vulnerable coastal areas. Building reliance on the protection and restoration of coastal mangroves, sea grass beds, saltmarshes, and other ecosystems we will further establish a coastal "buffer zone" to improve climate resilience and the adaptability of natural and social systems.

4. Conclusions

Based on the IPCC core concept of integrated climate change risk, a socio-economic vulnerability index was developed for China's coastal areas. This was applied to assess the spatial patterns and dynamic evolution of socio-economic vulnerability at the provincial, city, and county level in 2010, 2030, 2050, and 2100 based on low, medium, and high GHG emission scenarios (SSP1-2.6, SSP2-4.5, and SSP5-8.5, respectively). The following main conclusions can be drawn:

(1) Under the modeled scenarios, the socio-economic vulnerability of China's coastal provinces, cities, and counties shows a proportional upward trend, reaching peak vulnerability by 2100. This is associated with continued sea-level rise coupled with a declining labor force and reductions in adaptability.

(2) Based on the three SSP scenarios, the higher the degree of climate warming, the greater the rise in sea level along China's coast and, consequently, the greater the increase in socio-economic vulnerability and economic exposure. This is compounded by increasing sensitivity to coastal hazards associated with an aging population.

(3) At the provincial level, areas with high socio-economic vulnerability are concentrated in Tianjin around Bohai Bay, Shanghai, Jiangsu, and Zhejiang around the Yangtze River Delta, and Guangdong Province in the Pearl River Delta region. At the city and country level, the highest vulnerability areas are also concentrated in coastal cities and counties around Bohai Bay, the Yangtze River Delta, and the Pearl River Delta. Although these areas are economically developed and have high adaptability, they often have a high proportion of low-lying land and high levels of exposure owing to dense residential populations.

(4) The hazards posed by climate change disaster-causing factors can be reduced as follows: by controlling GHG emissions; strengthening the standards of damp-proofing, flood control, and land drainage; strengthening the industrial structure and layout of coastal low-lying areas; improving the observation, prediction, and early warning systems of sea-level rise. Collectively, these measures can reduce the exposure and vulnerability of coastal areas, and the protection and restoration of productive coastal ecosystems can also help improve the climate resilience and adaptability of China's coastal areas.

Coastal areas are a strategic focus of China's national economic and social development but are also prone to natural disasters. Climate change, high-density development, and a productive social economy make coastal areas vulnerable to the hazards of climate change, particularly sea-level rise. Therefore, it is urgent to identify vulnerable areas and formulate targeted adaptation and mitigation. Based on the results presented in this study, the Bohai Bay Rim, Yangtze River Delta, Jiangsu, and Pearl River Delta regions are highlighted as the most vulnerable coastal areas under projections up to 2100. To build on these findings, the current lack of simulation data for future levels of urbanization and education, medical care, and social security infrastructure needs to be addressed to facilitate the most robust projections. It is, therefore, necessary to further integrate multiple data indicators to optimize the developed socio-economic vulnerability index, which shows potential as a comprehensive risk-evaluation tool and for informing the development of targeted mitigation measures and adaptation strategies.

Author Contributions: Conceptualization, R.C., C.L. and X.Y.; methodology, C.L.; software, C.L. and X.Y.; validation, C.L. and R.C.; formal analysis, C.L.; investigation, R.C., C.L. and X.Y.; resources, C.L. and R.C.; data curation, C.L.; writing—original draft preparation, C.L.; writing—review and editing, C.L. and R.C.; visualization, C.L.; supervision, R.C.; project administration, R.C.; funding acquisition, C.L. All authors have read and agreed to the published version of the manuscript.

Funding: This research was funded by a Key Special Funding Project of the National Key R&D Plan, "Global Change and Response" (2017YFA0604902; 2017YFA0604904).

Institutional Review Board Statement: Not applicable.

Informed Consent Statement: Not applicable.

Data Availability Statement: Not applicable.

Acknowledgments: This work was supported by Zhang Hua, a senior engineer from the National Safety and Emergency Management School of Beijing Normal University, and we thank the research team for their future forecast data.

Conflicts of Interest: The authors declare no conflict of interest. The funders had no role in the design of the study; in the collection, analyses, or interpretation of data; in the writing of the manuscript; or in the decision to publish the results.

References

1. IPCC. *Climate Change 2021: The Physical Science Basis*; Masson-Delmotte, V., Zhai, P., Pirani, A., Connors, S.L., Péan, C., Chen, Y., Goldfarb, L., Gomis, M.I., Matthews, J.B.R., Berger, S., et al., Eds.; Contribution of Working Group I to the Sixth Assessment Report of the Intergovernmental Panel on Climate Change; Cambridge University Press: Cambridge, UK; New York, NY, USA, 2021.
2. Sung, H.M.; Kim, J.; Lee, J.-H.; Shim, S.; Boo, K.-O.; Ha, J.-C.; Kim, Y.-H. Future Changes in the Global and Regional Sea Level Rise and Sea Surface Temperature Based on CMIP6 Models. *Atmosphere* **2021**, *12*, 90. [CrossRef]
3. Oppenheimer, M.; Glavovic, B.; Hinkel, J. Sea Level Rise and Implications for Low Lying Islands, Coasts and Communities [M/OL]//IPCC. An IPCC Special Report on the Ocean and Cryosphere in a Changing Climate. 2019. Available online: https://www.ipcc.ch/srocc/home (accessed on 24 September 2019).
4. Cai, R.S.; Tan, H.J. Impacts and risks of accelerating sea level rise on low lying islands, coasts and communities. *Clim. Chang. Res.* **2020**, *16*, 163–171.
5. Zhang, T.; Yu, Y.Q.; Xiao, C.D.; Hua, L.-J.; Yan, Z. Interpretation of IPCC AR6 report: Monitoring and projections of global and regional sea level change. *Clim. Chang. Res.* **2022**, *18*, 12–18.
6. Marine Early Warning and Monitoring Department of the Ministry of Natural Resources. *China Sea Level Bulletin*; Ministry of Natural Resources of the People's Republic of China. 2022. Available online: https://www.mnr.gov.cn/sj/sjfw/hy/gbgg/zghpmgb/ (accessed on 20 September 2021).
7. Marine Early Warning and Monitoring Department of the Ministry of Natural Resources. *Bulletin of China Marine Disasters*; Ministry of Natural Resources of the People's Republic of China. 2021. Available online: https://www.mnr.gov.cn/sj/sjfw/hy/gbgg/zghyzhgb/ (accessed on 20 September 2021).
8. Hinkel, J.; Lincke, D.; Vafeidis, A.T.; Perrette, M.; Nicholls, R.J.; Tol, R.S.; Marzeion, B.; Fettweis, X.; Ionescu, C.; Levermann, A. Coastal flood damage and adaptation costs under 21st century sea-level rise. *Proc. Natl. Acad. Sci. USA* **2014**, *111*, 3292–3297. [CrossRef]
9. Kossin, J.P.; Knapp, K.R.; Olander, T.L.; Velden, C.S. Global increase in major tropical cyclone exceedance probability over the past four decades. *Proc. Natl. Acad. Sci. USA* **2020**, *117*, 11975–11980. [CrossRef]
10. Small, C.; Nieholls, R.J. A Global Analysis of Human Settlement in Coastal Zones. *J. Coast. Resour.* **2003**, *19*, 584–599.
11. Adger, W.N.; Hughes, T.P.; Folke, C.; Carpenter, S.R.; Rockstrom, J. Social-Ecological Resilience to Coastal Disaster. *Science* **2005**, *309*, 1036–1039. [CrossRef]
12. Ding, P. *Evolution Process and Cause Analysis of Typical Coastal Zone in China during the Last 50 Years*; Science Press: Beijing, China, 2013.

13. Fang, J.; Liu, W.; Yang, S.; Brown, S.; Nicholls, R.J.; Hinkel, J.; Shi, X.; Shi, P. Spatial—Temporal changes of coastal and marine disasters risks and impacts in Mainland China. *Ocean. Coast. Manag.* **2017**, *139*, 125–140. [CrossRef]
14. Xiao, R.; Guo, P.; Xie, X. Theoretical research of storm surge loss assessment. *Trans. Oceanol. Limnol.* **2021**, *43*, 68–73.
15. Cai, R.; Xu, W. Risk of socio-economic losses from floods in China's coastal cities. *China Popul. Resour. Environ.* **2022**, *32*, 174–184.
16. IPCC. *Climate Change 2014: Impacts, Adaptation, and Vulnerability: Contribution of Working Group II to the Fifth Assessment Report of the Intergovernmental Panel on Climate Change*; Cambridge University Press: Cambridge, UK, 2014; pp. 1–32.
17. IPCC. *Summary for Policymakers. [R/OL]//Climate Change 2022: Impacts, Adaptation, and Vulnerability*; Contribution of Working Group II to the Sixth Assessment Report of the Intergovernmental Panel on Climate Change; Cambridge University Press: Cambridge, UK, 2022. Available online: https://report.ipcc.ch/ar6wg2/pdf/IPCC_AR6_WGII_SummaryForPolicymakers.pdf (accessed on 5 May 2022).
18. Ekstrom, J.A.; Suatoni, L.; Cooley, S.R.; Pendleton, L.H.; Waldbusser, G.G.; Cinner, J.E.; Ritter, J.; Langdon, C.; van Hooidonk, R.; Gledhill, D.; et al. Vulnerability and adaptation of US shellfisheries to ocean acidification. *Nat. Clim. Chang.* **2015**, *5*, 207–214. [CrossRef]
19. Romieu, E.; Welle, T.; Schneiderbauer, S.; Pelling, M.; Vinchon, C. Vulnerability assessment within climate change and natural hazard contexts: Revealing gaps and synergies through coastal applications. *Sustain. Sci.* **2010**, *5*, 159–170. [CrossRef]
20. Cutter, S.L.; Boruff, B.J.; Shirley, W.L. Social Vulnerability to Environmental Hazards. *Soc. Sci. Q.* **2003**, *84*, 242–261. [CrossRef]
21. Yi, L.X.; Zhang, X.; Ge, L.L.; Dong, Z. Analysis of social vulnerability to hazards in China. *Environ. Earth Sci.* **2014**, *71*, 3109–3117.
22. Tierney, K. Social Inequality, Hazards, and Disasters. In *On Risk and Disaster Lessons from Hurricane Katrina*; Daniels, R.J., Kettl, D.F., Kunreuther, H., Eds.; Philadephia University of Pennsylvania Press: Philadephia, PA, USA, 2006; pp. 109–128.
23. Shi, J.G.; Yu, X.Y. Infrastructure Vulnerability Assessment and Spatial Analysis of the Yangtze River Delta Urban Agglomeration under Climate Change. *J. Tongji Univ. (Nat. Sci. Ed.)* **2020**, *48*, 1836–1844.
24. Hahn, M.B.; Riederer, A.M.; Foster, S.O. The livelihood vulnerability index: A pragmatic approach to assessing risks from climate variability and change: A case study in Mozambique. *Glob. Environ. Chang.* **2009**, *19*, 74–88. [CrossRef]
25. Fang, J.Y.; Chen, W.F.; Kong, F.; Sun, S.; Shi, P.J. Measuring social vulnerability to natural hazards of the coastal areas in China. *J. Beijing Norm. Univ. (Nat. Sci.)* **2015**, *51*, 280–286.
26. Cheng, S.B.; Yue, Y.; Liu, Y.; Yang, X.L. Evaluation and Analysis of the Social Vulnerability of Flood Disasters in the Yellow River Basin. *Yellow River* **2022**, *44*, 45–50.
27. Bjarnadottir, S.; Li, Y.; Stewart, M.G. Social vulnerability index for coastal communities at risk to hurricane hazard and a changing climate. *Nat. Hazards* **2011**, *59*, 1055–1075. [CrossRef]
28. Pandey, R.; Jha, S. Climate vulnerability index-measure of climate change vulnerability to communities: A case of rural Lower Himalaya, India. *Mitig. Adapt. Strateg. Glob. Chang.* **2012**, *17*, 487–506. [CrossRef]
29. Xu, T.; Xu, C.; Liu, Y. Research on Shanghai Comprehensive Vulnerability Assessment of Climate Change—Based on PSR Model. *Resour. Dev. Mark.* **2015**, *31*, 288–292.
30. Zhang, D.; Jiao, M. Vulnerability Assessment of Coastal Areas Development Based on RBF Neural Network. *J. Hebei Norm. Univ. (Nat. Sci. Ed.)* **2019**, *43*, 446–452.
31. Qin, X. Spatial Characteristics and Evaluation of Regional Vulnerability of Marine Meteorological Disasters in Coastal Cities of Guangxi. *Pop. Sci. Technol.* **2020**, *22*, 20–23.
32. Cutter, S.L.; Finch, C. Temporal and spatial changes in social vulnerability to natural hazards. *Proc. Natl. Acad. Sci. USA* **2008**, *105*, 2301–2306. [CrossRef]
33. Hizbaron, D.R.; Baiquni, M.; Sartohadi, J.; Rijanta, R.; Coy, M. Assessing social vulnerability to seismic hazard through spatial multi criteria evaluation in Bantul District, Indonesia. In Proceedings of the Conference of Development on the Margin, Bonn, Germany, 5–7 October 2011; Volume 10, pp. 5–7.
34. Depietri, Y.; Welle, T.; Renaud, F.G. Social vulnerability assessment of the Cologne urban area to heat waves: Links to ecosystem services. *Int. J. Disaster Risk Reduct.* **2013**, *6*, 98–117. [CrossRef]
35. Zheng, D.F.; Gao, M.; Li, Y.; Wu, R.N. Comprehensive risk assessment of rainstorm-flood disaster in Dalian City based on GIS. *J. Hohai Univ. (Nat. Sci.)* **2022**, *50*, 22.
36. Huang, X.J.; Huang, X.; Cui, C.L.; Yang, X.J. Concept, analysis framework and evaluation method of social vulnerability. *Prog. Geogr.* **2014**, *33*, 1512–1525.
37. Jiao, M.; Zhang, D.Y. The Vulnerability Assessment on the Development of the Coastal Area in the Context of Sea Level Rise. *J. Cap. Norm. Univ. (Nat. Sci. Ed.)* **2019**, *40*, 41–47.
38. Wang, J.; Wang, W.A.; Wang, S.F. Climate Change and Coastal Vulnerability Assessment: A Case Study of China's Yangtze River Delta Region. *Geomat. Spat. Inf. Technol.* **2017**, *40*, 81–89.
39. Huang, J.; She, J.W. Vulnerability Assessment and Influencing Factors Analysis of Urban Flood Disaster in Yangtze River Delta City Cluster. *J. Hohai Univ. (Philos. Soc. Sci.)* **2020**, *22*, 39–45.
40. China Statistical Yearbook. National Bureau of Statistics of the People's Republic of China. Available online: http://www.stats.gov.cn/tjsj/ndsj/ (accessed on 20 October 2021).
41. Kopp, R.E.; Horton, R.M.; Little, C.M.; Mitrovica, J.X.; Oppenheimer, M.; Rasmussen, D.J.; Strauss, B.H.; Tebaldi, C. Probabilistic 21st and 22nd century sea—Level projections at a global network of tide—Gauge sites. *Earth's Future* **2014**, *2*, 383–406. [CrossRef]

42. Zhang, H.; Li, X.M.; Li, W.L. Data Set of Coastal Population, Urban Expansion and Land Use under the Future Path of SSPs. Available online: https://nsem.bnu.edu.cn/gjgcs/120719.htm (accessed on 24 October 2021).
43. Zhang, H.; Li, X.M.; Dong, L.J. GDP Data Set of Coastal Areas under the Future Path of SSPs. Available online: https://nsem.bnu.edu.cn/gjgcs/120719.htm (accessed on 24 October 2021).
44. Chen, Q.; Hu, Q.G. The vulnerability evaluation and influencing factors of the socio-ecological system of China's marine fisheries. *Res. Agric. Mod.* **2018**, *39*, 468–477.
45. Yan, X.H.; Cai, R.; Guo, H.; Xu, W.; Tan, H. Vulnerability of Hainan Dongzhaigang mangrove ecosystem to the climate change. *J. Appl. Oceanogr.* **2019**, *38*, 338–349.
46. Shi, M.Q. Study on the Population Spatial Distribution and Its Natural Disaster Vulnerability in China's Low Elevation Coastal Zone. Master's thesis, Shanghai Normal University, Shanghai, China, 2012.
47. Li, X.; Duan, X.; Zhang, Z.; Wang, H.; Liu, K.X. The Vulnerability Zoning Research on the Sea Level Rise of Chinese Coastal. *J. Catastrophology* **2016**, *31*, 103–109.
48. Yuan, S.; Zhao, X.; Li, L.L. Combination evaluation and case analysis of vulnerability of storm surge in coastal provinces of China. *Acta Oceanol. Sin.* **2016**, *38*, 16–24.
49. Gao, C.; Wang, L.; Chen, C.; Luo, G.; Sun, Y. Population and economic risk exposure in coastal regionof China under sea level rise. *Acta Geogr. Sin.* **2019**, *74*, 1590–1604.
50. Morzaria-Luna, H.N.; Turk-Boyer, P.; Moreno-Baez, M. Social indicators of vulnerability for fishing communities in the Northern Gulf of California, Mexico: Implications for climate change. *Mar. Policy* **2014**, *45*, 182–193. [CrossRef]
51. Cinner, J.E.; McClanahan, T.R.; Graham, N.A.; Daw, T.M.; Maina, J.; Stead, S.M.; Wamukota, A.; Brown, K.; Bodin, Ö. Vulnerability of coastal communities to key impacts of climate change on coral reef fisheries. *Glob. Environ. Chang.* **2012**, *22*, 12–20. [CrossRef]
52. Yu, L.P.; Pan, Y.T.; Wu, Y.S. Research on sensitivity analysis of science and technology evaluation—Single index and combined index. *Soft Sci.* **2009**, *23*, 1–4.
53. Yang, Y.; Fang, G.H.; Huang, X.F.; Xu, S. Evaluation of the strictest regional water resources management based on improved fuzzy matter-element analysis. *Water Resour. Prot.* **2014**, *30*, 19–24.
54. Yu, W.Y. Comprehensive evaluation of regional social economic system vulnerability in Hebei province. *J. Yanshan Univ. (Philos. Soc. Sci. Ed.)* **2012**, *13*, 64–66.
55. Xu, W.H.; Cai, R.S. Estimating the return period of extreme water level in coastal cities of China under different climate scenarios. *Mar. Sci. Bull.* **2022**, *41*, 379–390.
56. Zhu, F. Analysis on the trend of population aging in China's coastal areas under the SSP scenario. *Reg. Gov.* **2021**, *8*, 63–64. [CrossRef]